Electronic Supplementary Information

Quinoxaline-based thermally activated delayed fluorescence emitters for highly efficient organic light emitting diode

Xiaoning Li[a], Yi Chen[a], Shuhui Li[d], Aisen Li[e], Liangjing Tu[a], Dongdong Zhang*[b], Lian Duan[b], Yujun Xie*[a], Ben Zhong Tang*[ac], Zhen Li*[adef]

[a]Institute of Molecular Aggregation Science, Tianjin University, Tianjin, 300072, China
E-mail: xieyujun@tju.edu.cn.
[b]Key Lab of Organic Optoelectronics and Molecular Engineering of Ministry of Education, Department of Chemistry, Tsinghua University Beijing 100084, China
E-mail: ddzhang@mail.tsinghua.edu.cn
[c]Shenzhen Institute of Molecular Aggregate Science and Engineering, School of Science and Engineering, The Chinese University of Hong Kong, Shenzhen, 2001 Longxiang Boulevard, Longgang District, 518172 Shenzhen City, Guangdong, China.
E-mail: tangbenz@cuhk.edu.cn
[d]Department of Chemistry, Wuhan University, Wuhan, Hubei, 430072, China.
E-mail: lizhen@whu.edu.cn.
[e]Joint School of National University of Singapore and Tianjin University, International Campus of Tianjin University Binhai New City, Fuzhou, Fujian, 350207, China
[f]Wuhan National Laboratory for Optoelectronics, Huazhong University of Science and Technology, Wuhan 430074, China

Contents

1. CV curves of Br-TTPZ and NMR Spectra

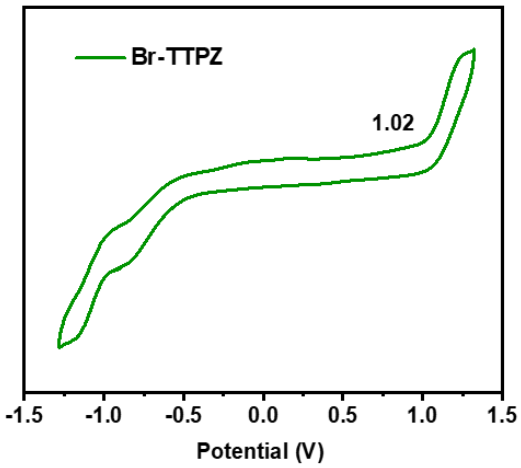

Figure **S1.** Cyclic voltammogram of Br-TTPZ.

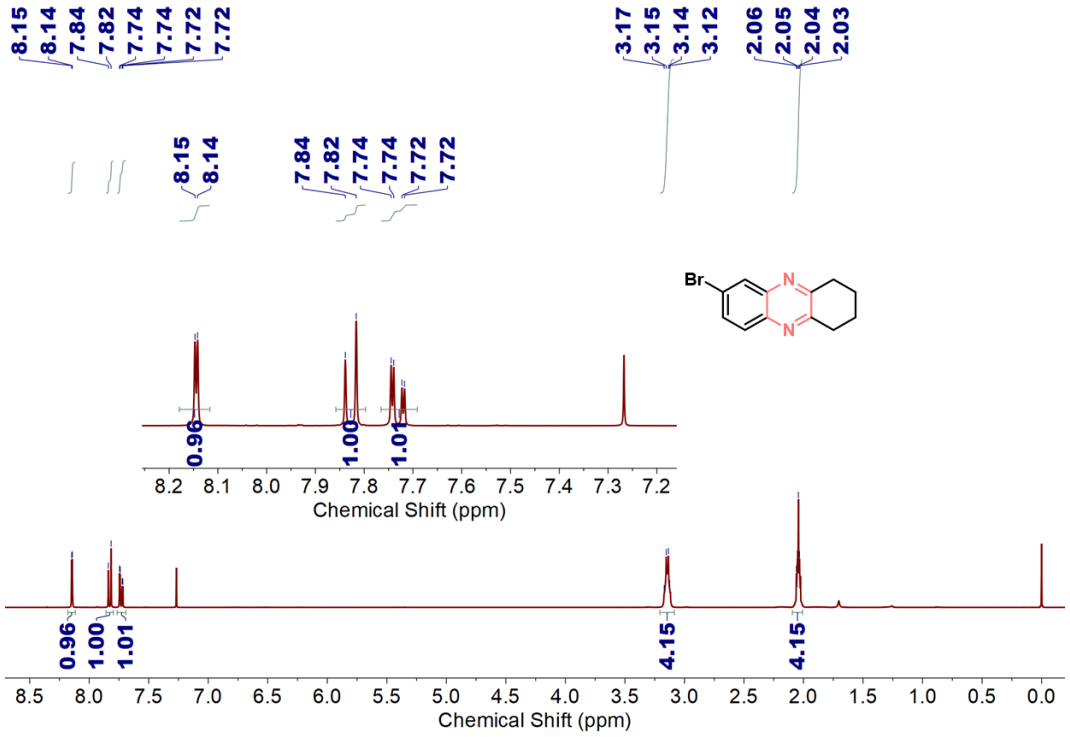

Figure S2. ^{1}H NMR spectrum of Br-TTPZ.

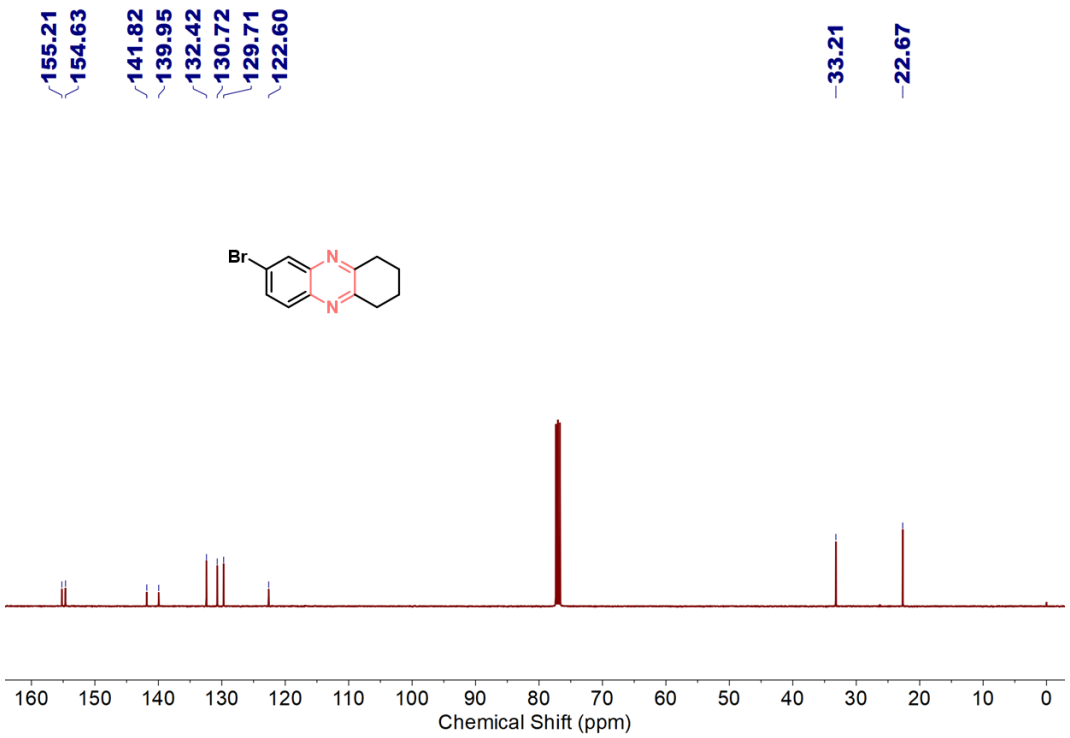

Figure S3. ^{13}C NMR spectrum of Br-TTPZ.

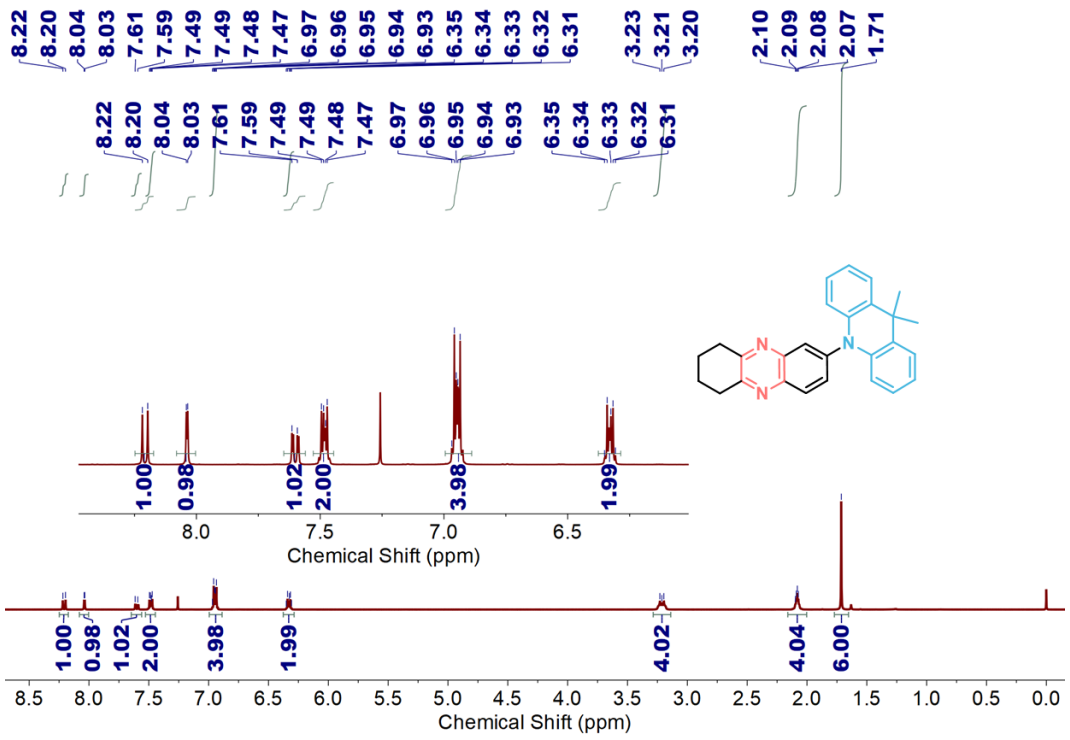

Figure S4. ^{1}H NMR spectrum of DMAC-TTPZ.

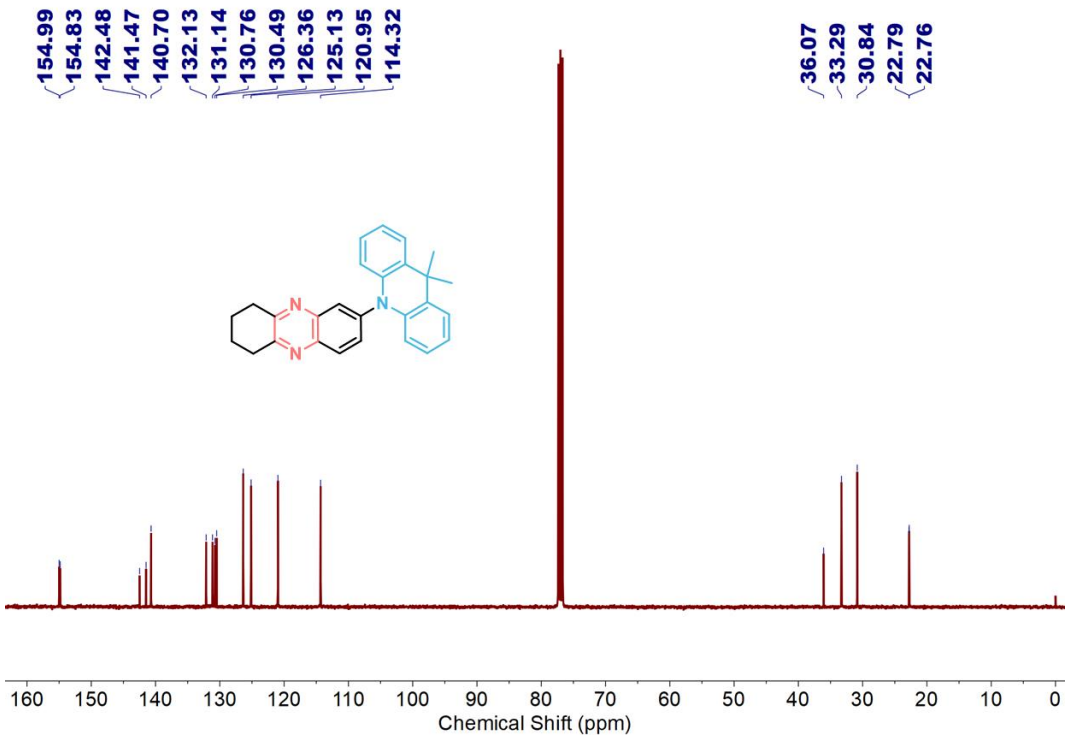

Figure S5. ^{13}C NMR spectrum of DMAC-TTPZ.

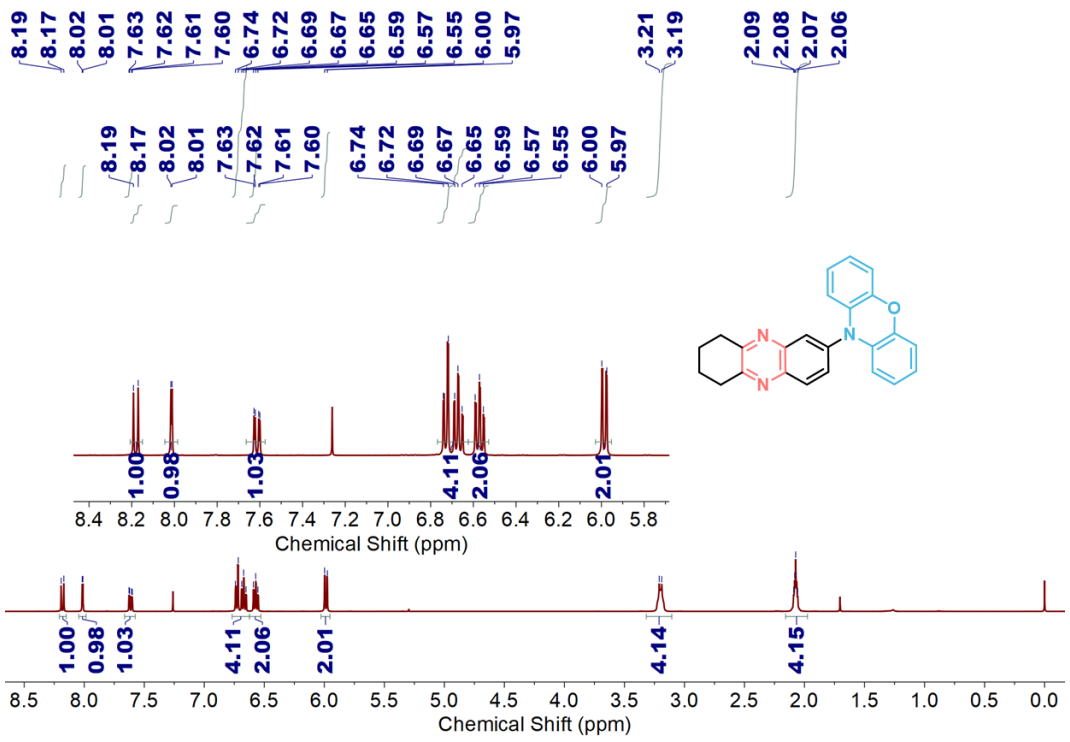

Figure S6. ^{1}H NMR spectrum of PXZ-TTPZ.

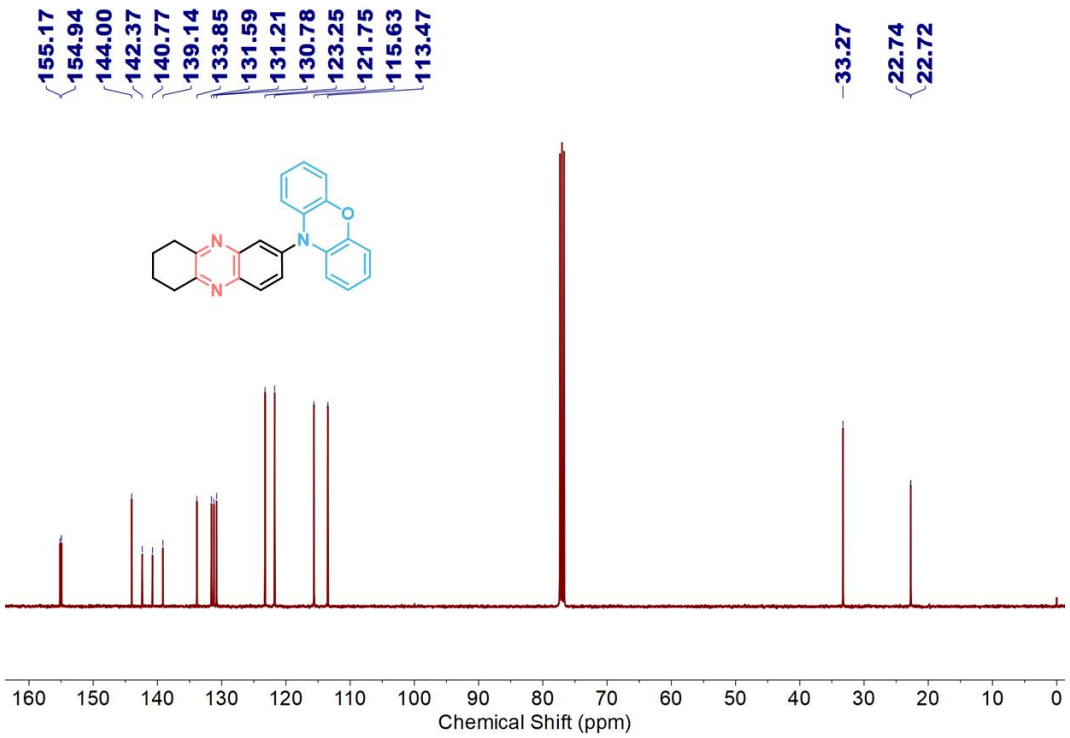

Figure S7. ^{13}C NMR spectrum of PXZ-TTPZ.

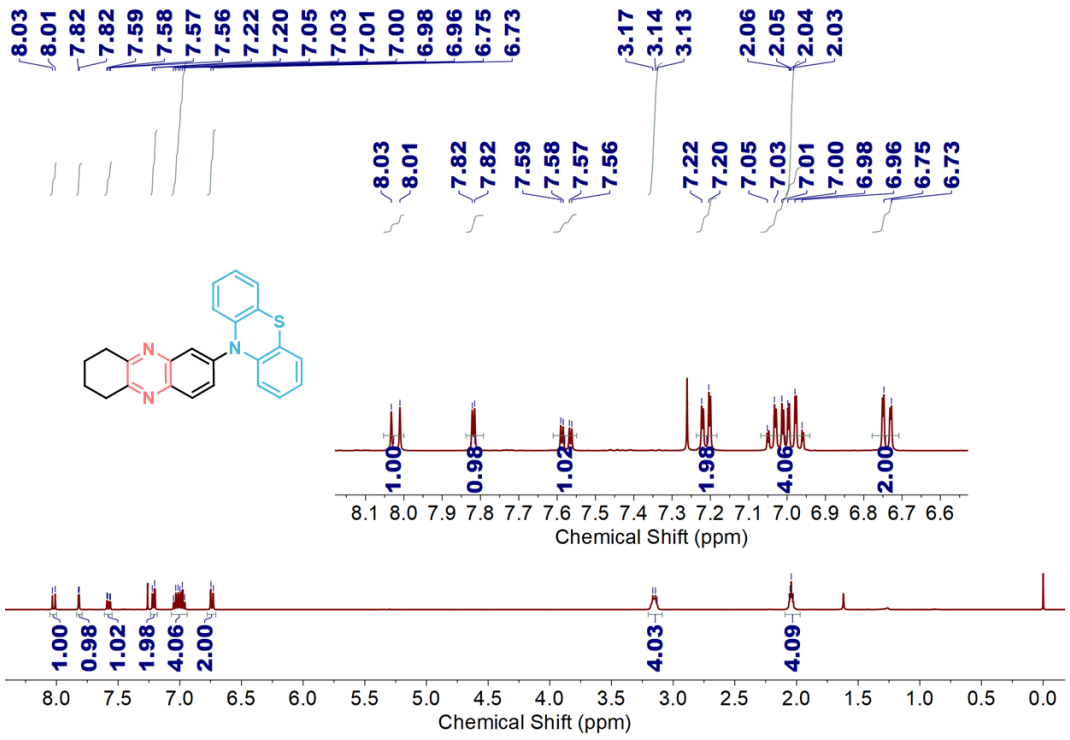

Figure S8. ^{1}H NMR spectrum of PTZ-TTPZ.

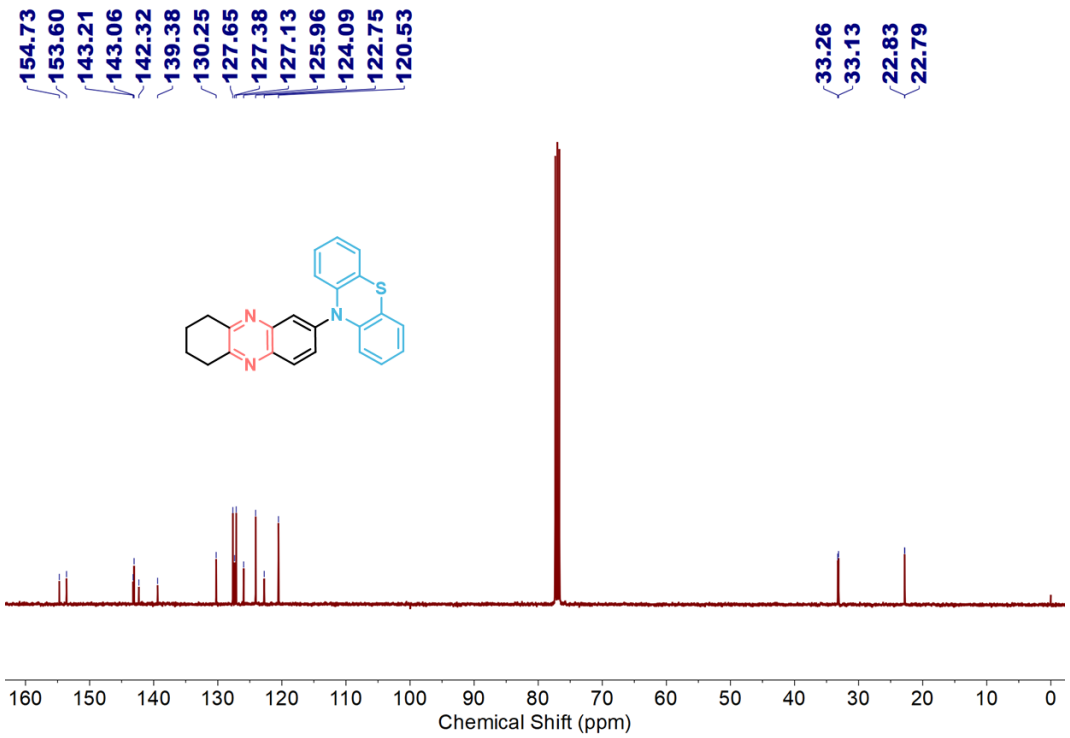

Figure S9. ^{13}C NMR spectrum of PTZ-TTPZ.

2. HRMS Spectra

Mass Spectrum SmartFormula Report

Analysis Info

Analysis Name	D:\Data\IAC TEST\DATA\QTOF-YUANWAI\LI Zhen\20220812\DMAC-TTPZ_P1-A-2_01_2837.d	Acquisition Date	8/12/2022 11:20:34 AM
Method	tune_wide_20220812.m	Operator	XZ/YSY
Sample Name	DMAC-TTPZ	Instrument / Ser#	microtof Q II 10387
Comment			

Acquisition Parameter

Source Type	ESI	Ion Polarity	Positive	Set Nebulizer	0.8 Bar
Focus	Active	Set Capillary	4500 V	Set Dry Heater	180 °C
Scan Begin	150 m/z	Set End Plate Offset	-500 V	Set Dry Gas	4.0 l/min
Scan End	3000 m/z	Set Collision Cell RF	400.0 Vpp	Set Divert Valve	Source

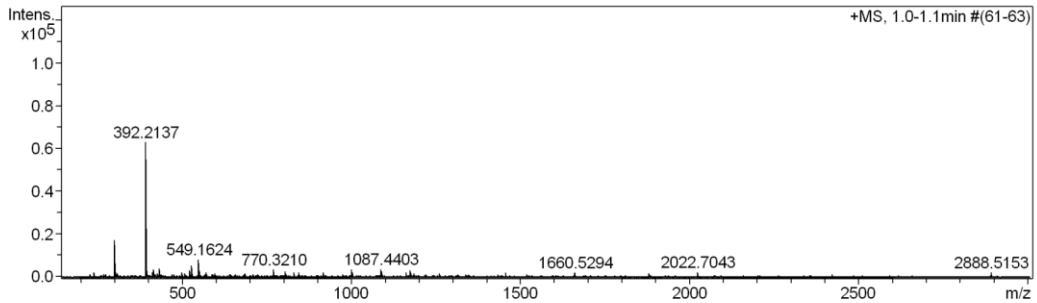

Meas. m/z	#	Formula	Score	m/z	err [mDa]	err [ppm]	mSigma	rdb	e⁻ Conf	N-Rule
392.2137	1	C 27 H 26 N 3	100.00	392.2121	-1.5	-3.9	21.9	16.5	even	ok

Figure S10. HRMS spectrum of DMAC-TTPZ.

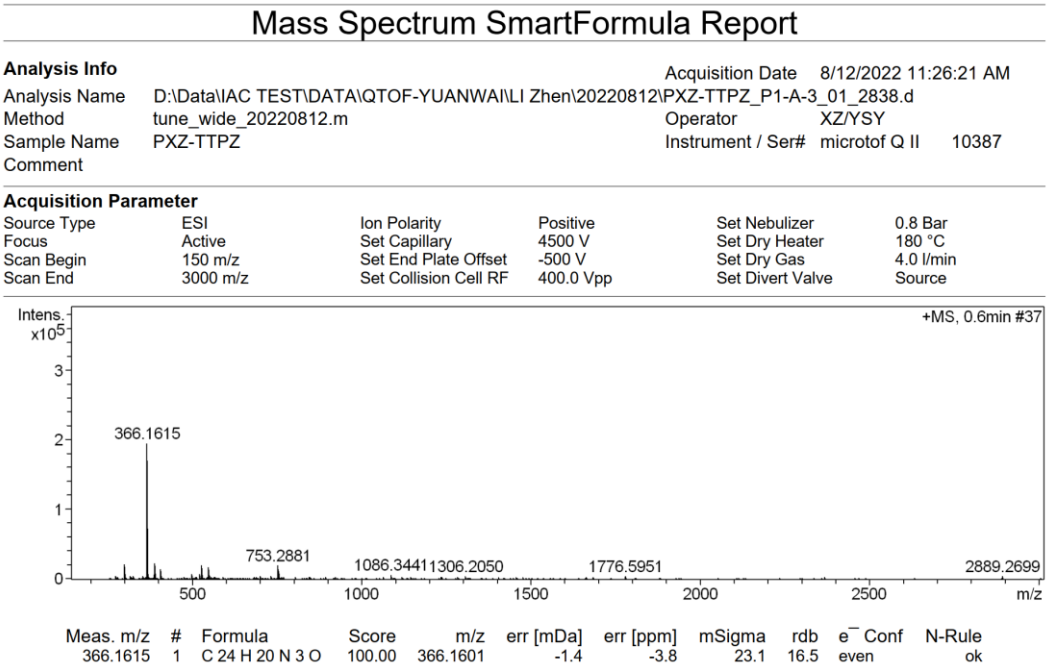

Figure S11. HRMS spectrum of PXZ-TTPZ.

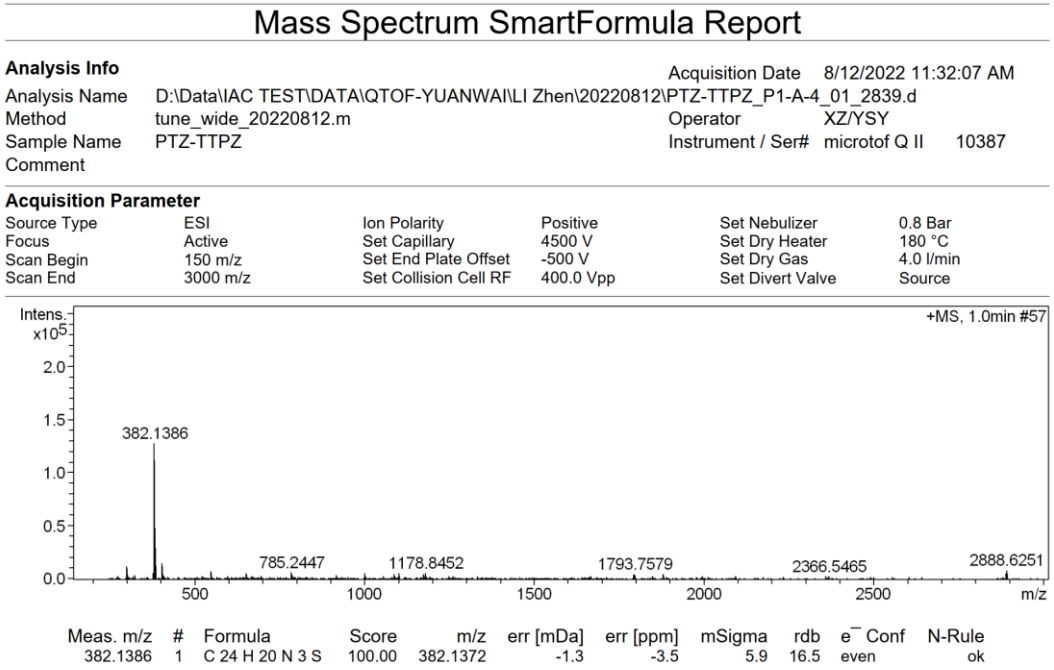

Figure S12. HRMS spectrum of PTZ-TTPZ.

3. DSC Voltammogram

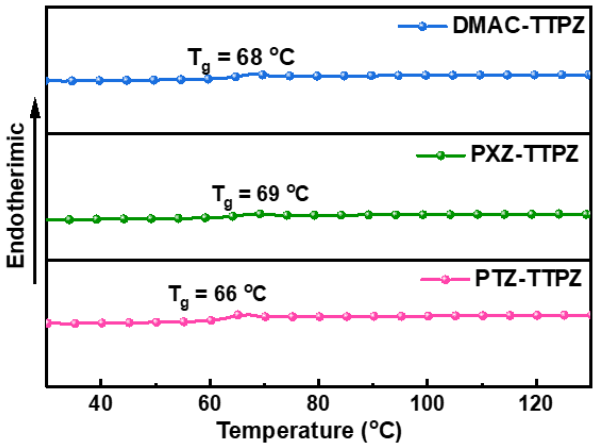

Figure **S13**. DSC voltammogram of DMAC-TTPZ, PXZ-TTPZ, and PTZ-TTPZ.

4. Photophysical Properties

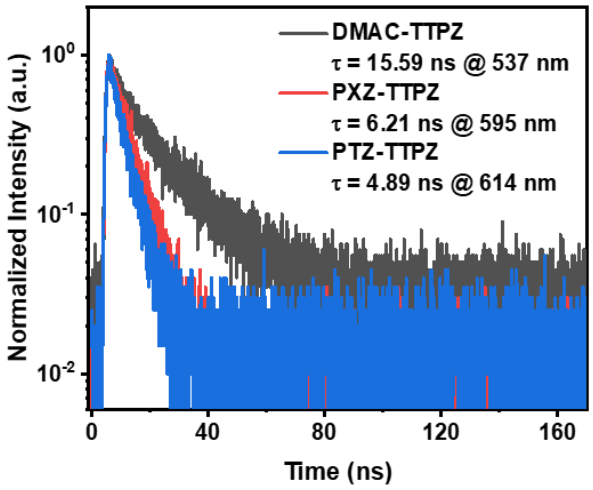

Figure **S14**. Time-resolved PL decay curves of DMAC-TTPZ, PXZ-TTPZ, and PTZ-TTPZ in toluene solution (5×10^{-5} mol L^{-1}) under N_2 atmosphere.

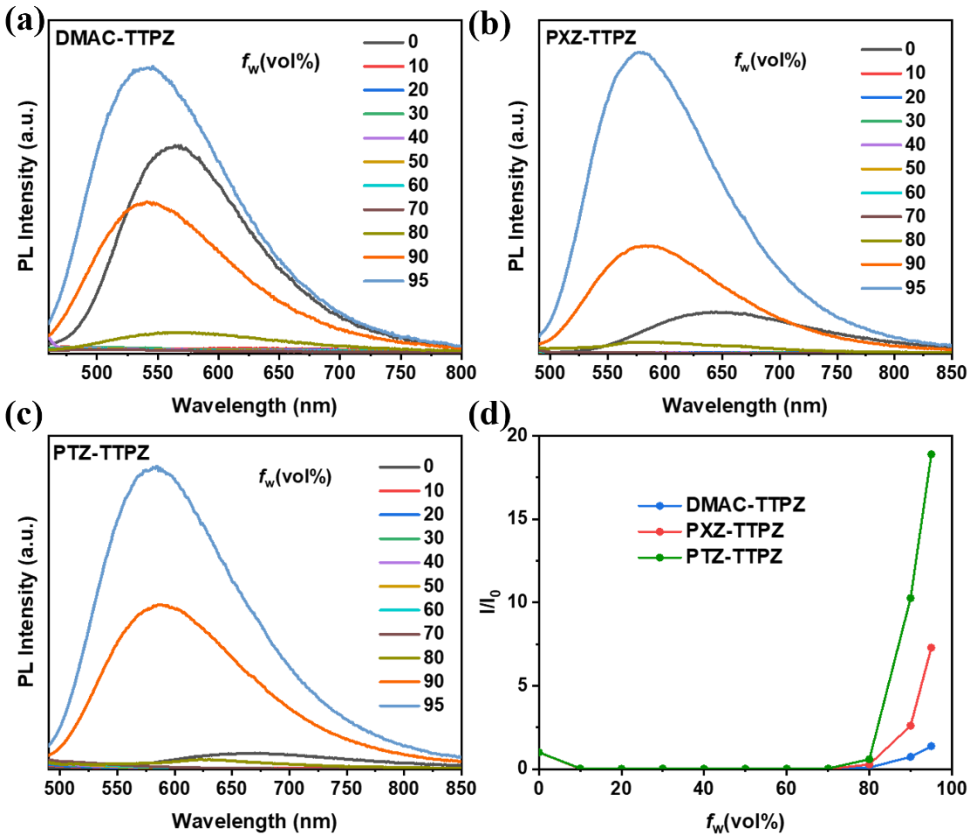

Figure **S15**. PL spectra of DMAC-TTPZ (a), PXZ-TTPZ (b), and PTZ-TTPZ (c) in THF-water mixtures with different water fractions (f_W). Concentration: 5 × 10^{-5} mol L-1. (d) Plots of I/I_0 versus f_w for DMAC-TTPZ, PXZ-TTPZ, and PTZ-TTPZ. I_0 is the PL intensity in pure THF solution.

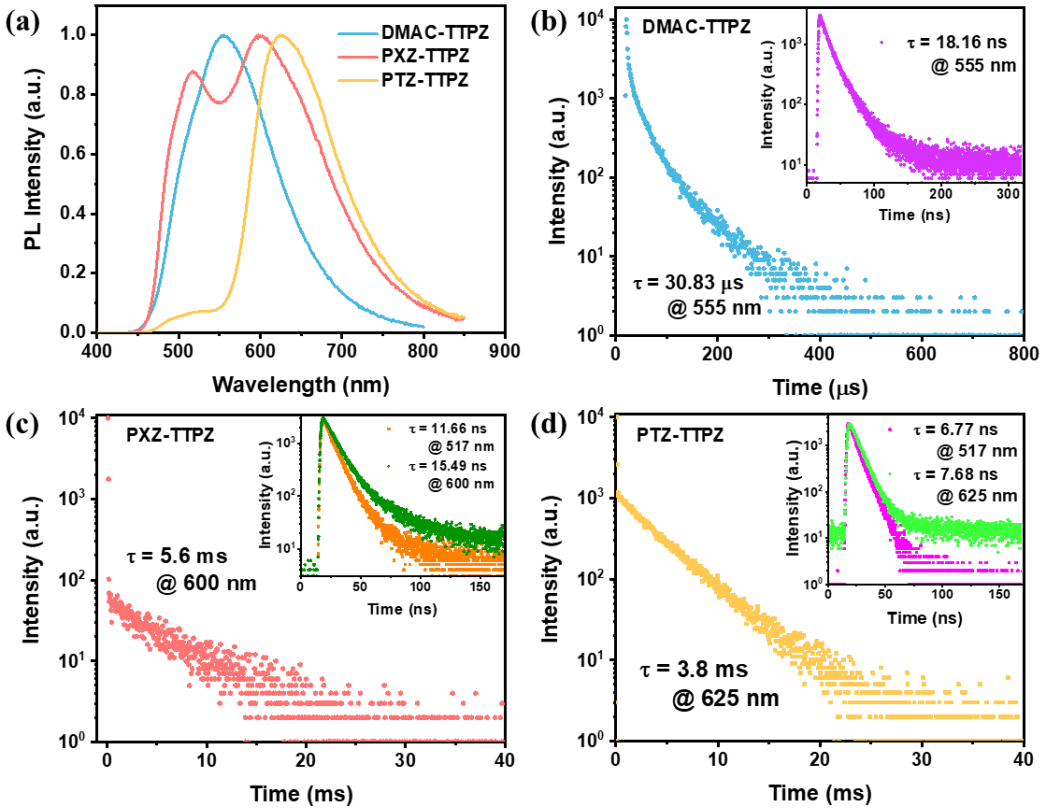

Figure **S16.** PL spectra (a) and time-resolved PL decay curves of DMAC-TTPZ (b), PXZ-TTPZ (c), and PTZ-TTPZ (d) in the solid state.

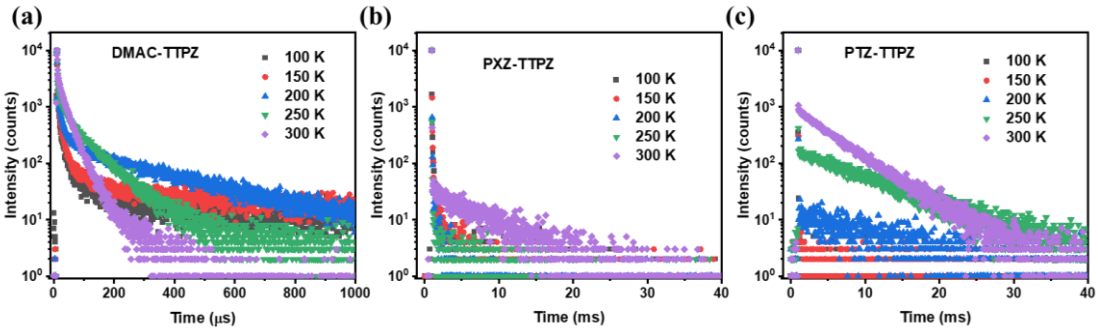

Figure **S17.** Time-resolved PL decay curves of DMAC-TTPZ (d), PXZ-TTPZ (e), and PTZ-TTPZ (f) in the solid state at different temperatures.

Table S1. Photodynamic parameter of PXZ-TTPZ.

Compound	k_p [s^{-1}]	k_d [s^{-1}]	k_r [s^{-1}]	k_{ISC} [s^{-1}]	k_{RISC} [s^{-1}]
PXZ-TTPZ	4.4×10^{7}	1.0×10^{5}	9.5×10^{6}	2.6×10^{7}	2.5×10^{5}

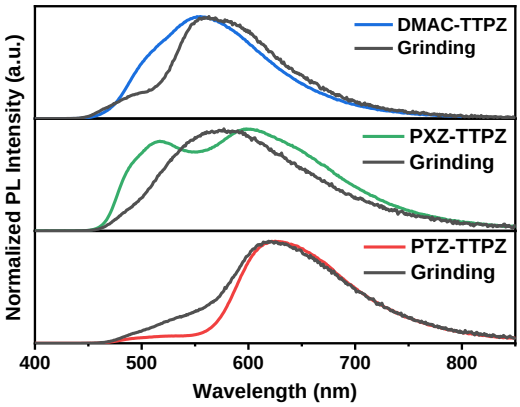

Figure **S18.** PL spectra of DMAC-TTPZ, PXZ-TTPZ, and PTZ-TTPZ before and after grinding.

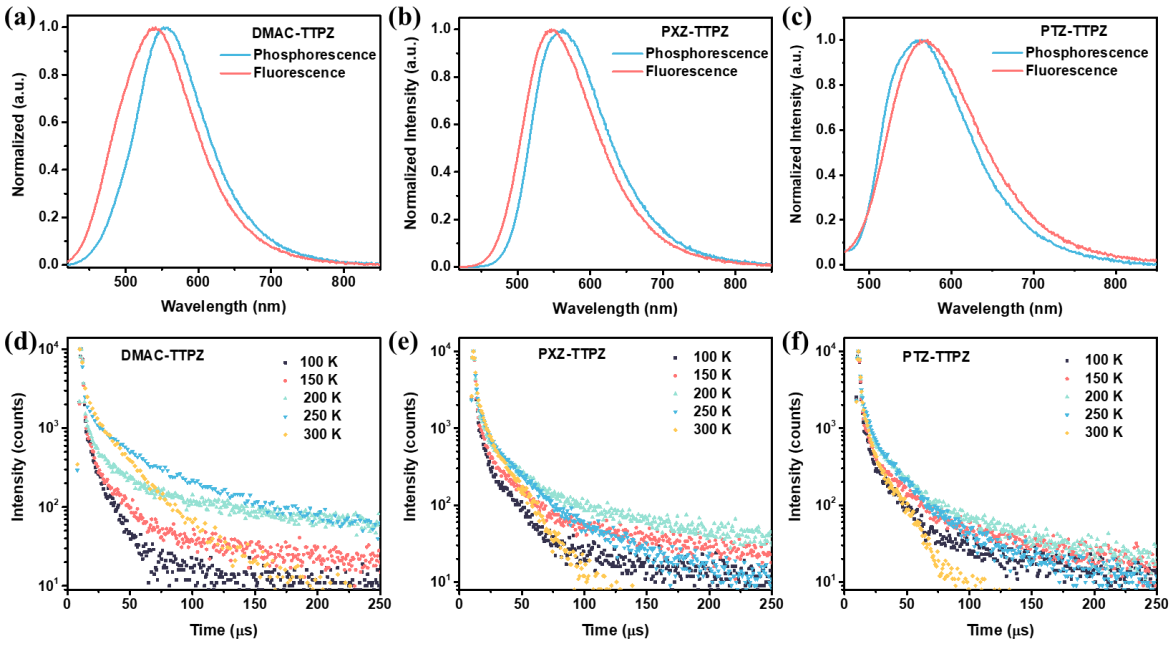

Figure **S19.** Fluorescence (298 K) and phosphorescence (77 K) spectra of DMAC-TTPZ (a), PXZ-TTPZ (b), and PTZ-TTPZ (c) in the doped PMMA film (5 wt%). Time-resolved PL decay curves of DMAC-TTPZ (d), PXZ-TTPZ (e), and PTZ-TTPZ (f) in the doped PMMA film (5 wt%) at different temperatures.

5. Device Performances

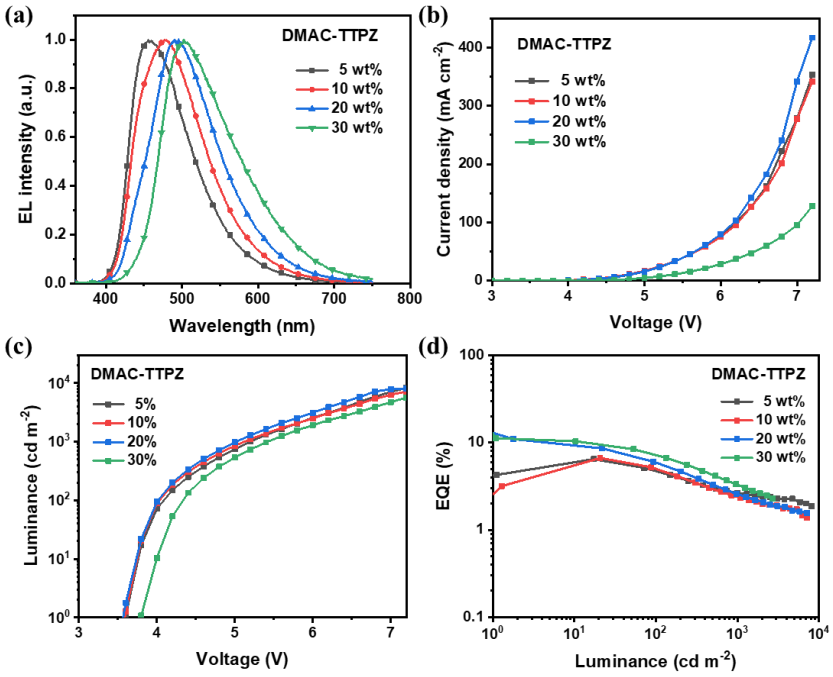

Figure **S20.** EL spectra (a), current density (b) and luminance (c) as a function of voltage, and EQE versus luminance of DMAC-TTPZ with different doping ratios in OLEDs.

Table S2. Summary of OLED characteristics based on DMAC-TTPZ.

Concentration (wt%)	V_{on} (V)	EQE_{max} (%)	PE_{max} (lm W^{-1})	CIE	λ_{max} (nm)	FWHM (nm)
5	3.6	6.5	11.9	(0.18, 0.21)	456	90
10	3.6	6.7	13.5	(0.19, 0.28)	478	104
20	3.6	11.0	23.5	(0.23, 0.37)	490	102
30	3.8	11.2	22.1	(0.29, 0.46)	502	111

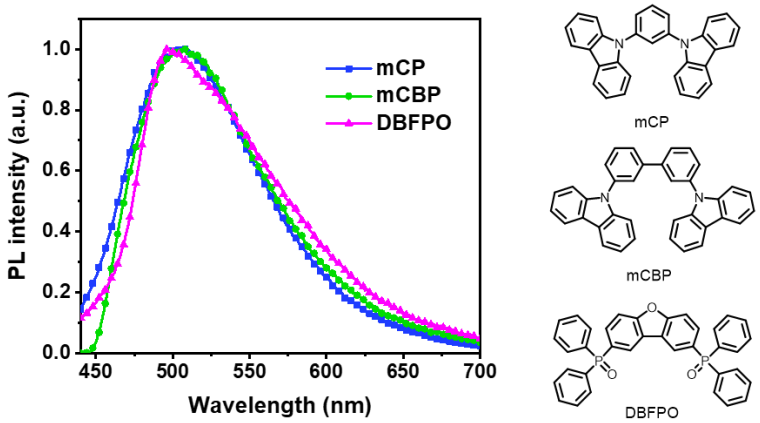

Figure **S21.** PL spectra of DMAC-TTPZ doped in mCP, mCBP, and DBFPO (5 wt%).

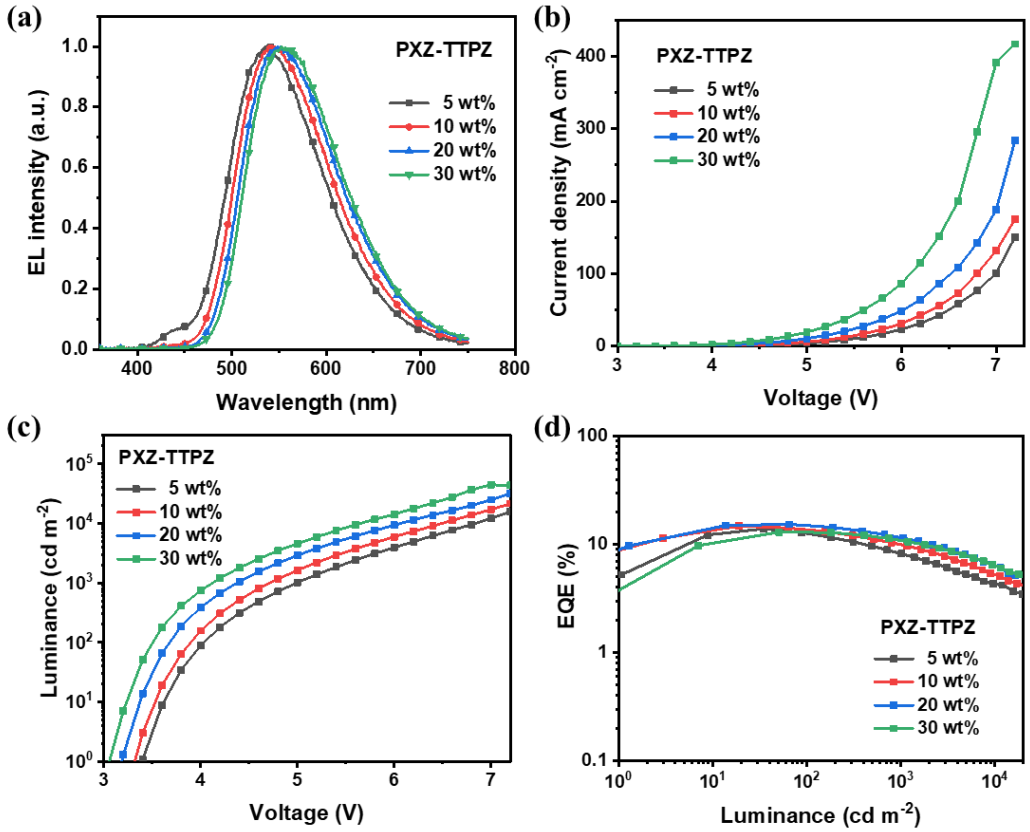

Figure **S22.** EL spectra (a), current density (b) and luminance (c) as a function of voltage, and EQE versus luminance of PXZ-TTPZ with different doping ratios in OLEDs.

Table S3. Summary of OLED characteristics based on PXZ-TTPZ.

Concentration (wt%)	V_{on} (V)	EQE_{max} (%)	PE_{max} (lm W^{-1})	CIE	λ_{max} (nm)	FWHM (nm)
5	3.4	13.9	35.5	(0.36, 0.53)	536	113
10	3.4	14.8	39.1	(0.39, 0.55)	546	114
20	3.2	15.3	41.0	(0.42, 0.54)	551	116
30	3.2	13.0	35.2	(0.43, 0.54)	553	116

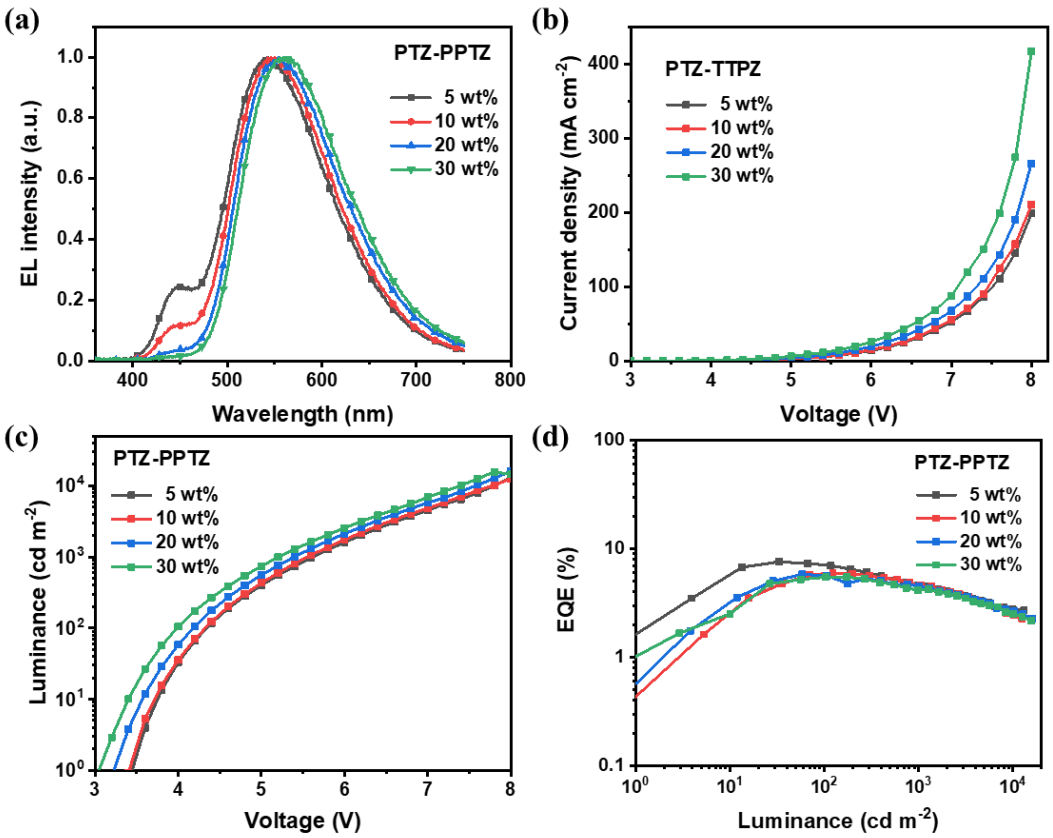

Figure **S23.** EL spectra (a), current density (b) and luminance (c) as a function of voltage, and EQE versus luminance of PTZ-TTPZ with different doping ratios in OLEDs.

Table S4. Summary of OLED characteristics based on PTZ-TTPZ.

Concentration (wt%)	V_{on} (V)	EQE_{max} (%)	PE_{max} (lm W^{-1})	CIE	λ_{max} (nm)	FWHM (nm)
5	3.6	7.6	17.3	(0.36, 0.48)	542	121
10	3.6	6.0	12.4	(0.39, 0.51)	546	121
20	3.4	5.8	12.8	(0.42, 0.53)	554	125
30	3.2	5.5	11.8	(0.44, 0.53)	567	126